Electronic Supplementary information for

Mild selective oxidative cleavage of lignin C-C bonds over copper catalyst in water

Yuzhen Hu, [a,c] Long Yan, [a] Xuelai Zhao,[d] Chenguang Wang, *[a,d] Song Li, [a,c] Xinghua Zhang, [a,b] Longlong Ma [a,b] and Qi Zhang *[a,b]

[a] Guangdong Provincial Key Laboratory of New and Renewable Energy Research and Development, CAS Key Laboratory of Renewable Energy, Guangzhou Institute of Energy Conversion, Chinese Academy of Sciences, Guangzhou 510640, PR China.

[b] Key Laboratory of Energy Thermal Conversion and Control of Ministry of Education, School of Energy and Environment, Southeast University, Nanjing 210096, PR China.

[c] University of Chinese Academy of Sciences, Beijing 100049, PR China

[d] Department of Thermal Science and Energy Engineering, University of Science and Technology of China, Hefei, 233022, PR China.

*Corresponding Author: zhangqi@ms.giec.ac.cn, wangcg@ms.giec.ac.cn.

Table of Contents

1. Chemicals and materials

CuCl (99.95%), CuBr (98%), Cu_2O (99%), $CuCl_2$ (99%), CuO (99%), $Cu(OAc)_2$ (98%), $Cu(OH)_2$ (94%), $CuSO_4$ (99%), $FeCl_3$ (99%), $MnCl_2$ (99%), $AlCl_3$ (97%), $ZnCl_2$

(98%), NaOH (98%), KOH (95%), Na_2CO_3 (99%), K_2CO_3 (99%), $CsCO_3$ (99%), $NH_3 \cdot H_2O$ (25-28%) and NaOAc (99%) were all purchased from Meryer (Shanghai) Co., Ltd. Dichloromethane (99%), hydrochloric acid (37%), anhydrous Na_2SO_4 (99%), 1,2-Diphenylethanone (98%), Diphenylethanedione (98%), 2-Hydroxy-1-phenylethanone (98%), phenyl formate (>97%), phenol (99.5%), 2-bromoacetophenone (99%), and acetone (99%) were all purchased from Shanghai Macklin Biochemical Co., Ltd. D_2O (99.5%) and DMSO-d_6 (99.9%) were purchased from Shanghai Aladdin Biochemical Technology Co., Ltd. All analytical reagent chemicals were used as received without further purification.

Corn stover was obtained from Mengcheng City, Anhui Province of China. Pine wood, eucalyptus wood, bagasse and bamboo were produced in South China. Compositional analysis of these samples was performed based on NREL's Laboratory Analytical Procedure (see Table S3).[1]

2. Products analysis and calculation of yields

2.1 Products analysis

The aromatic products were characterized and quantified using gas chromatography/mass spectrometer (GC-MS, Agilent 7890A-5975C) and gas chromatography (GC, Shimadzu GC-2010 Pro). A 1 μL injection volume was used through a 30 m × 250 μm × 0.25 μm column (Rtx-SH-5) with a split ratio of 30:1. An inlet temperature of 280 °C and an oven temperature of 80 °C with a 10 $^{o}C\ min^{-1}$ ramp to 280 °C was used with an overall run time of 32 min. ^{1}H, ^{13}C nuclear magnetic resonance （NMR）and two-dimensional heteronuclear single quantum coherence nuclear magnetic resonance （2D HSQC-NMR）spectra were obtained using a Bruker AVANCE III 400 MHz spectrometer at room temperature. Fourier transformation infrared (FT-IR) spectra was recorded by a Thermo Scientific Nicolet 6700 spectrometer. Solid sample was diluted with KBr and pressed into disc before FT-IR test.

2.2 Calculation of the conversion of lignin (models) and yield of products

Calculation of the conversion of lignin models (**a** represents β-O-4 models and **b** represents β-1 models) and yield of products (**c** represents benzoic acid and its derivatives; **d** represents phenol and its derivatives; **e** represents benzaldehyde and its derivatives):

$$Conversion\ of\ model\ a\ (\%) = \frac{Moles\ of\ reacted\ model\ a}{Moles\ of\ added\ a} \times 100\%$$

$$Conversion\ of\ model\ b\ (\%) = \frac{Moles\ of\ reacted\ model\ b}{Moles\ of\ added\ b} \times 100\%$$

$$Yield\ of\ product\ c\ (\%) = \frac{Moles\ of\ formed\ c}{Moles\ of\ added\ model} \times 100\%$$

$$Yield\ of\ product\ d\ (\%) = \frac{Moles\ of\ formed\ d}{Moles\ of\ added\ model} \times 100\%$$

$$Yield\ of\ product\ e\ (\%) = \frac{Moles\ of\ formed\ e}{Moles\ of\ added\ model} \times 100\%$$

Calculation of the yield of aromatic compounds from authentic lignin:

$$Yield\ of\ aromatic\ monomer\ \ (wt\%) = \frac{Mass\ of\ formed\ aromatic\ monomer}{Mass\ of\ starting\ lignin} \times 100\ wt\%$$

$$Vanillin\ Selectivity\ (\%) = \frac{Mass\ of\ Vanillin}{Mass\ of\ \ aromatic\ monomers} \times 100\%$$

$$Syringaldehyde\ Selectivity\ (\%) = \frac{Mass\ of\ Syringaldehyde}{Mass\ of\ aromatic\ monomers} \times 100\%$$

3. Synthesis and characterization of lignin models

Preparation of 2-phenoxy-1-phenylethanone (1a)

2-Phenoxy-1-phenylethanone was prepared by reference.[2] To a solution of phenol (2.4 g, 25 mmol) and K_2CO_3 (3.5 g, 25 mmol) in acetone (50 mL) was added 2-bromoacetophenone (4.7g, 23 mmol) with Ar atmosphere protection and was stirred at RT for 16 h. After reaction, the suspension was filtered and concentrated in vacuum. The solid was dissolved in ethyl acetate and washed with NaOH aqueous and water successively. The organic phase was then dried by anhydrous Na_2SO_4. The crude product was recrystallized from ethanol to give 2-phenoxy-1-phenylethanone as a white

solid in 78% yield. For the other methoxy substituted β-O-4 compounds, the procedures are the same as described above, except that different stating materials were used.

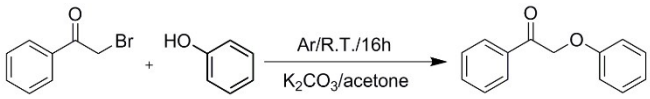

Procedure for the preparation of deuterium labelled 1a-d_2

The deuterated compound (Model 1a-d_2) was synthesized according to following procedure: 2-phenoxy-1-phenylethanone (1.1 g, 5.0 mmol) and anhydrous K_2CO_3 (0.1 g, 0.5 mmol) were added into D_2O (10 mL) in a 25 mL round bottom flask under argon atmosphere. The mixture was refluxed in an oil bath at 100 °C for 12 h. After cooling down to room temperature, the solvent was replaced by fresh D_2O under argon atmosphere, and further refluxed at 100 ºC for another 12 h. Then the obtained solid was washed to remove K_2CO_3 residues. Finally, the solid was dried under vacuum to give a deuterated compound as a light yellow solid.

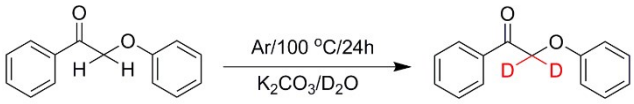

The structures of these compounds are confirmed by ^{1}H NMR (Fig. S1-S6).

1H NMR and 13C NMR:

Model **1a**: 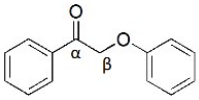

2-phenoxy-1-phenylethanone.

White solid.^{1}H NMR (400 MHz, DMSO-d6) δ 8.03-8.05 (t, J = 7.3 Hz, 2H), 7.68-7.72 (t, J = 7.4 Hz, 1H), 7.56-7.60 (t, J = 7.7 Hz, 2H), 7.26-7.32 (m, 2H), 6.93-6.99 (m, 3H), 5.58 (s, 2H). ^{13}C NMR (101 MHz, DMSO-d_6) δ = 195.11, 158.39, 134.90, 134.25, 129.89, 129.31, 128.34, 121.34, 115.08, 70.50.

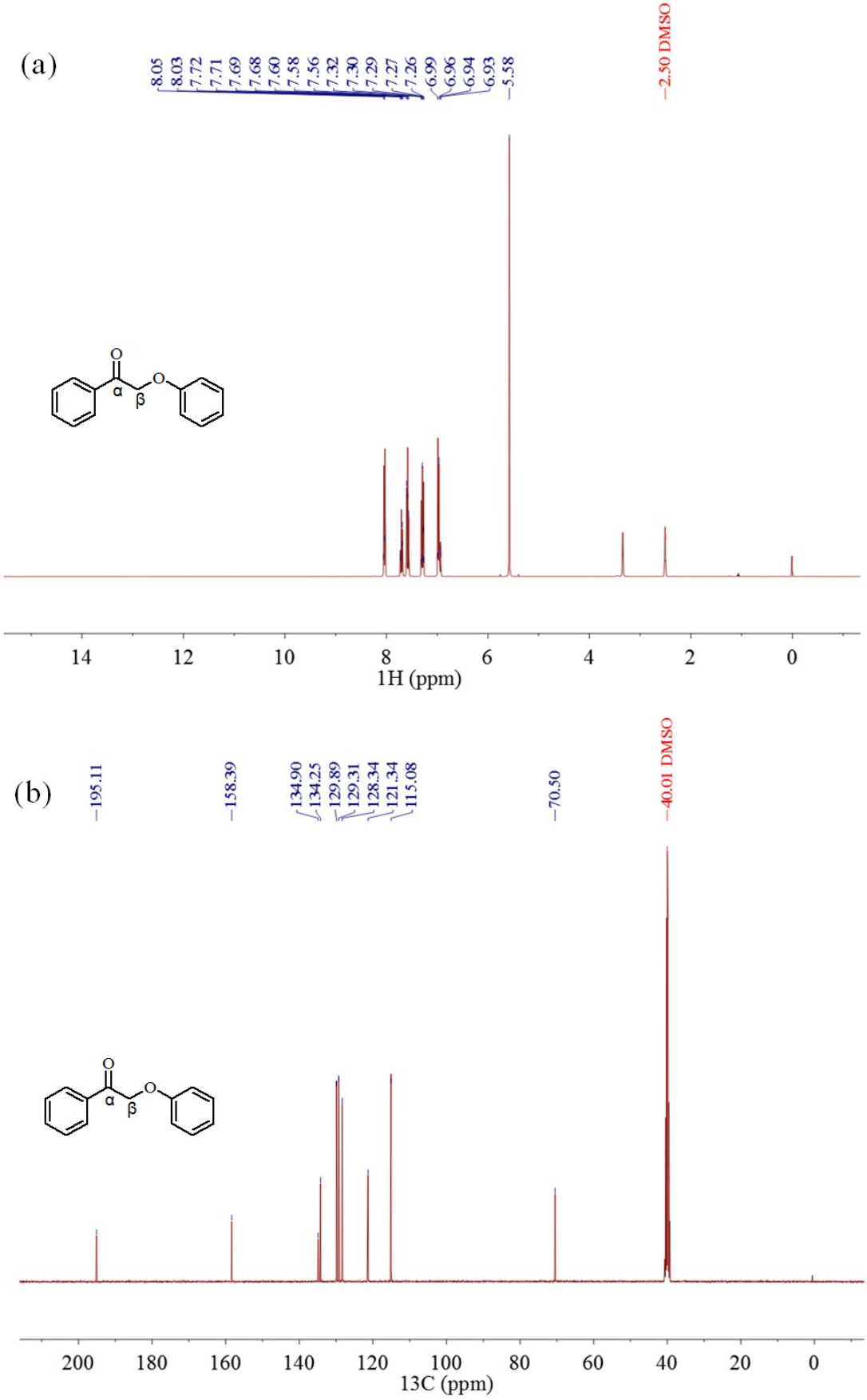

Fig. S1 ^{1}H NMR and ^{13}C NMR spectra of model 1a

Model 1a-d2: 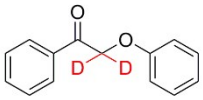 2-phenoxy-1-phenylethanone.

Light yellow solid. ^{1}H NMR (400 MHz, DMSO-d_6) δ 8.03-8.06 (t, J = 7.3 Hz, 2H), 7.68-7.73 (t, J = 7.4 Hz, 1H), 7.56-7.60 (t, J = 7.7 Hz, 2H), 7.26-7.31 (m, 2H), 6.93-6.99 (m, 3H). ^{13}C NMR (101 MHz, DMSO-d_6) δ = 195.21, 158.39, 134.91, 134.26, 129.89, 129.31, 128.35, 121.32, 115.07.

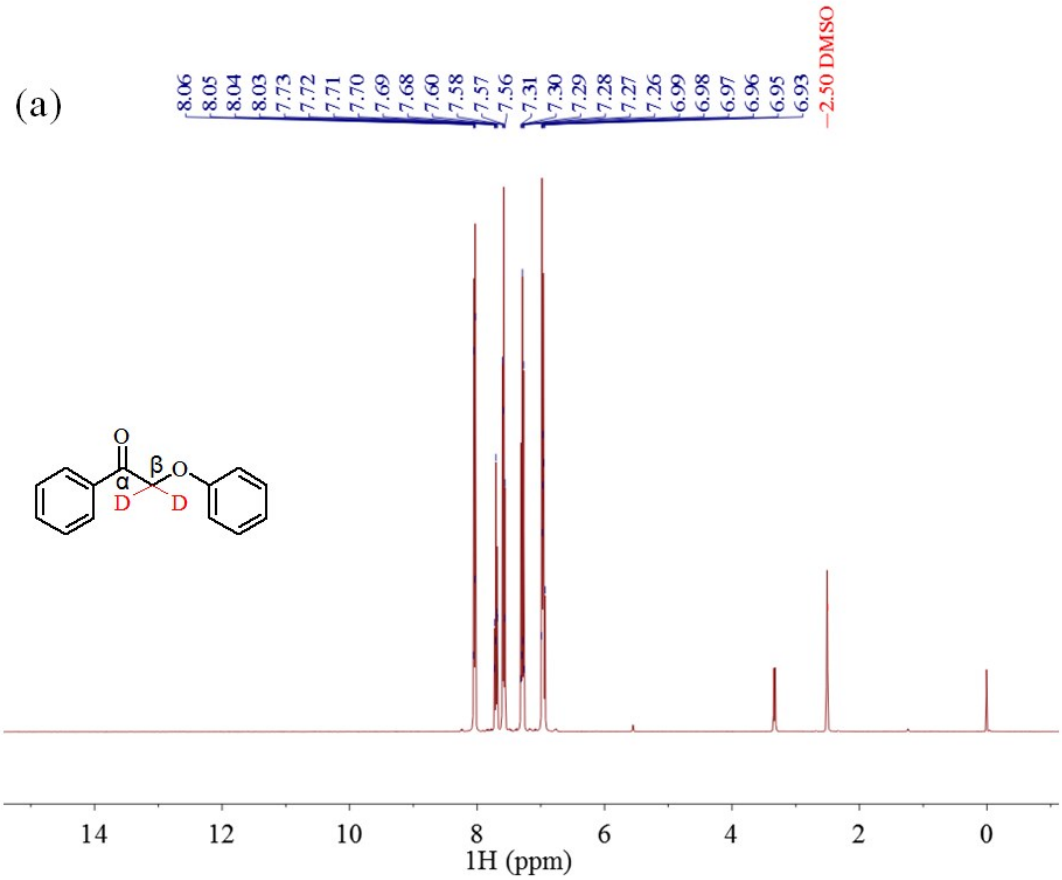

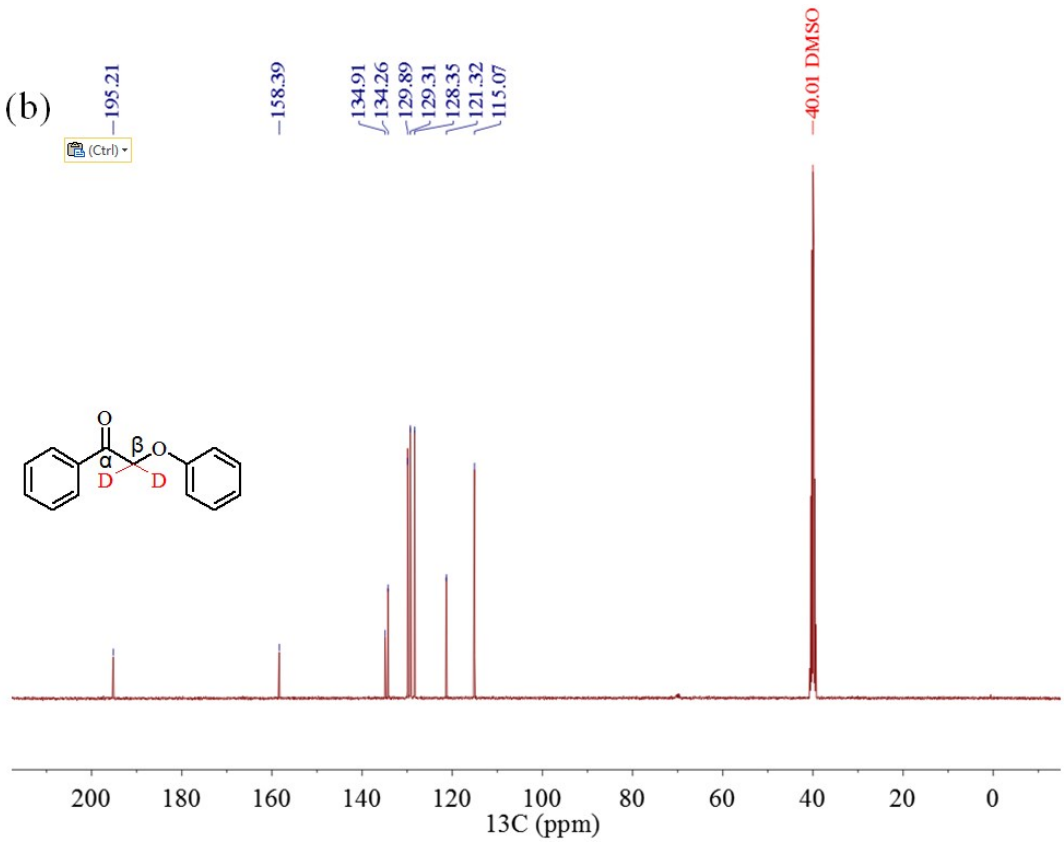

Fig. S2 ^{1}H NMR and ^{13}C NMR spectra of model 1a-d$_2$

Model 2a: 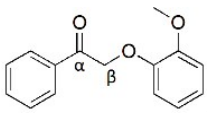

2-(2-methoxyphenoxy)-1-phenyl-ethanone.

White solid.^{1}H NMR (400 MHz, DMSO-d$_6$) δ 8.03-8.04 (t, J = 7.4 Hz, 2H), 7.68-7.72 (t, J = 7.4 Hz, 1H), 7.55-7.59 (t, J = 7.8 Hz, 2H), 6.89-7.01 (m, 2H), 6.81-6.85 (m, 3H), 5.54 (s, 2H), 3.79(s, 3H). ^{13}C NMR (101 MHz, DMSO-d$_6$) δ = 195.20, 149.47, 147.91, 134.94, 134.21, 129.29, 128.36, 121.84, 121.02, 114.21, 112.96, 71.23, 56.03.

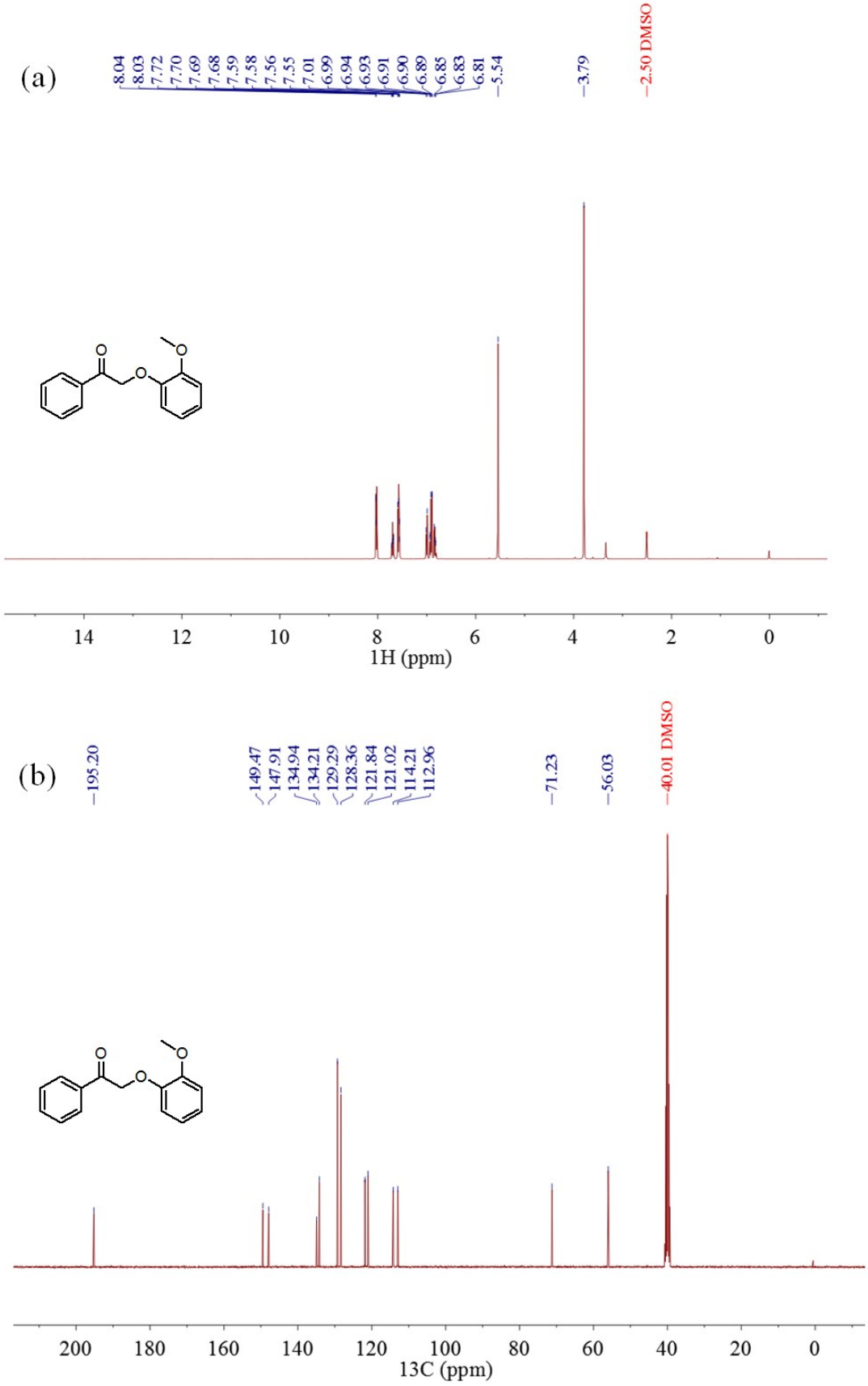

Fig. S3 ^{1}H NMR and ^{13}C NMR spectra of model 2a

Model 3a: 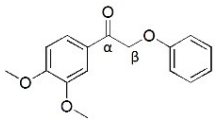 1-(3,4-dimethoxyphenyl)-2-phenoxyethanone.

Light yellow solid. .^{1}H NMR (400 MHz, DMSO-d_6) δ = 7.72-7.74 (dd, J = 8.4 Hz, 1.9, 1H),7.50 (d, J = 1.9 Hz, 1H), 7.26-7.31 (m, 2H), 6.93 –7.12(m, 4H), 5.51 (s, 2H), 3.84-3.87(d, J = 8.5 Hz, 6H). ^{13}C NMR (101 MHz, DMSO-d6) δ = 193.47, 158.48, 154.02, 149.19, 129.87, 127.72, 123.07, 121.27, 115.09, 111.50, 110.63, 70.24, 56.30, 56.06.

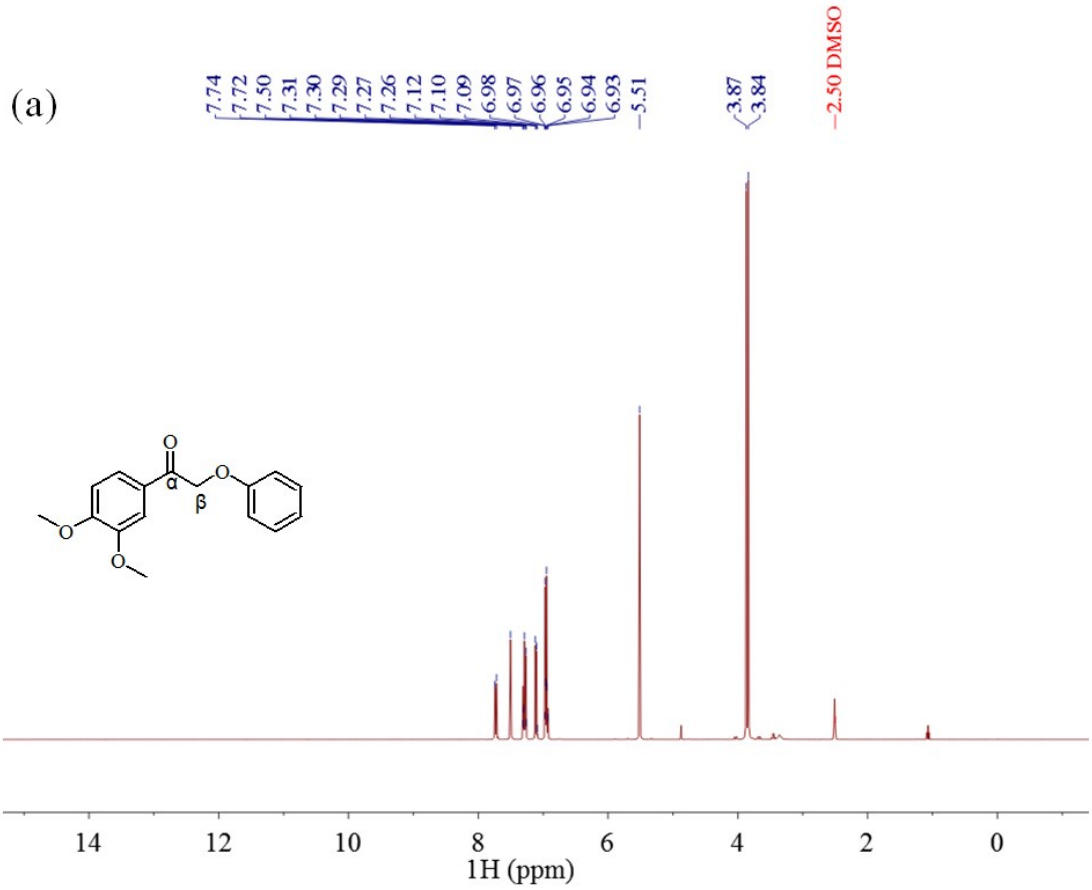

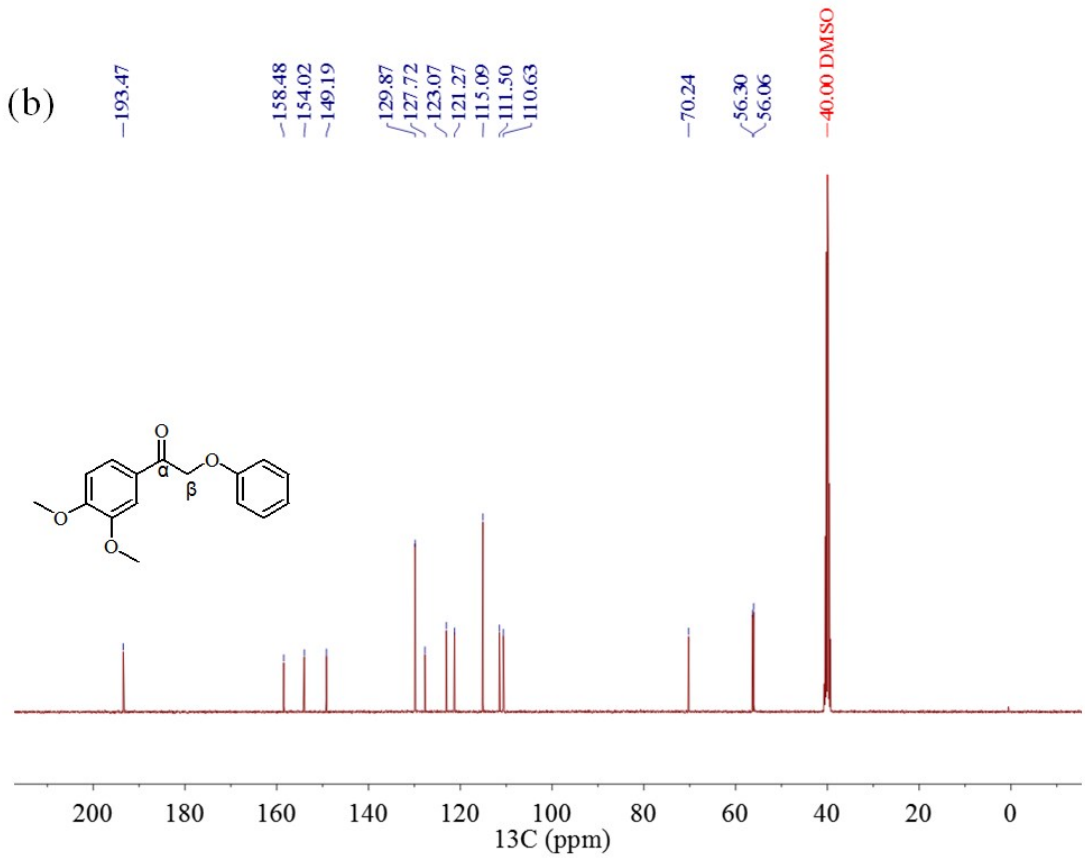

Fig. S4 ^{1}H NMR and ^{13}C NMR spectra of model 3a

Model **4a**: 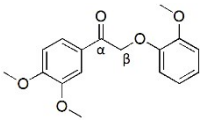 1-(3,4-dimethoxyphenyl)-2-(2-methoxyphenoxy)ethanone. White solid. ^{1}H NMR (400 MHz, DMSO-d_6) δ 7.72 (d, J = 8.4 Hz, 1H), 7.51 (d, J = 2.0 Hz, 1H), 7.11 (d, J = 8.5 Hz, 1H), 6.99 (dd, J = 8.0, 1.5 Hz, 2H), 6.96 – 6.78 (m, 2H), 5.47 (s, 2H), 3.85 (d, J = 12.6 Hz, 9H). ^{13}C NMR (101 MHz, DMSO-d_6) δ = 193.58, 153.99, 149.46, 149.16, 147.99, 127.76, 123.08, 121.78, 121.00, 114.15, 112.95, 111.48, 110.70, 71.01, 56.29, 56.03.

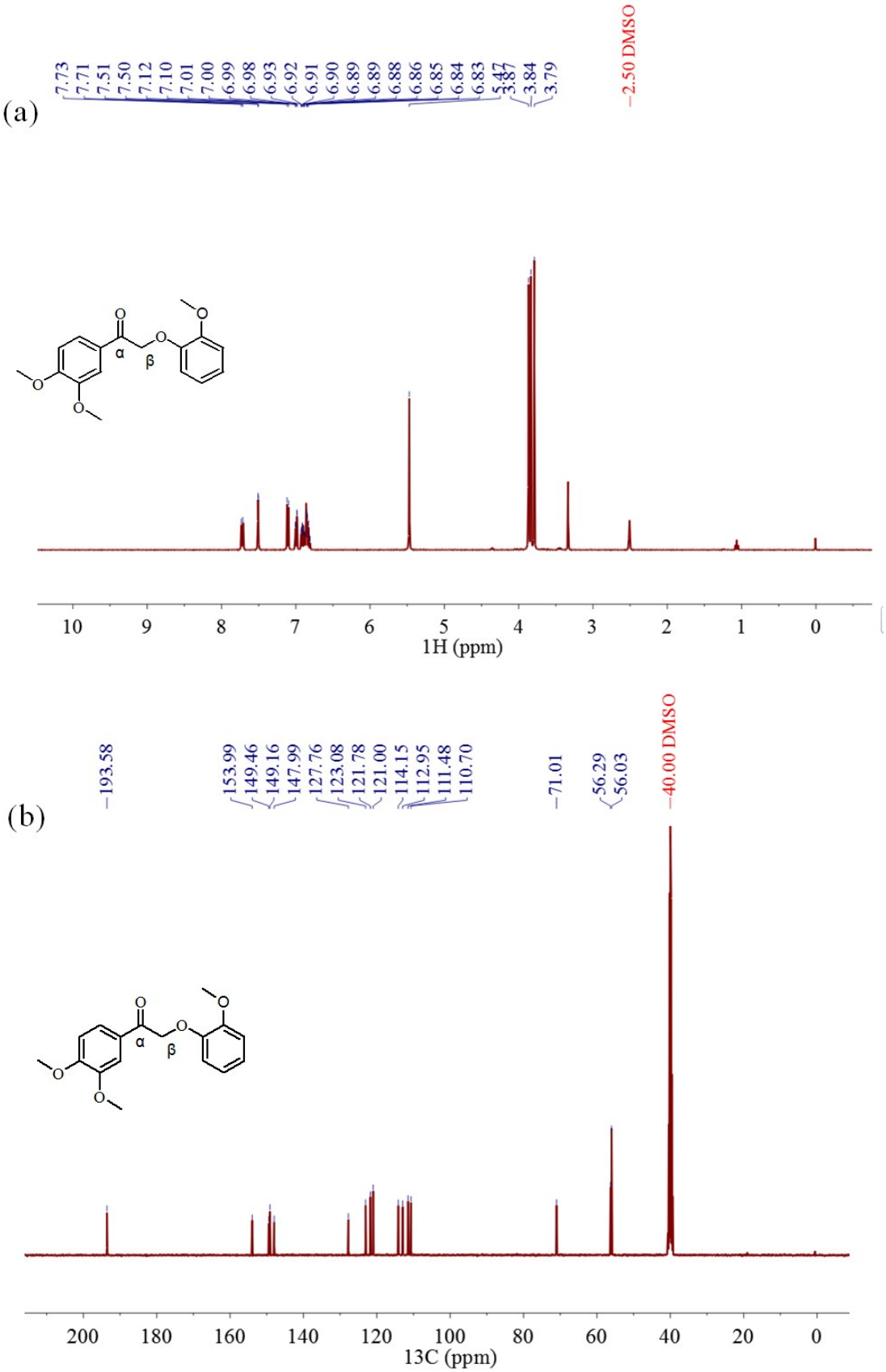

Fig. S5 ^{1}H NMR and ^{13}C NMR spectra of model 4a

Model **5a**: 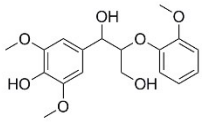

1-(4-Hydroxy-3,5-dimethoxyphenyl)-2-(2-methoxyphenoxy) propane-1,3-diol

Light yellow solid. ^{1}H NMR (400 MHz, DMSO-d_6) δ = 8.11 (s, 1H), 6.99 (dd, J =7.4, 2.2 Hz, 5H), 6.99-6.75 (m, 3H), 6.68(s, 2H), 5.33 (d, J = 4.7 Hz, 1H), 4.71(t, J = 5.0 Hz, 1H), 4.60(t, J = 5.6 Hz, 1H), 4.33 (q, J = 5.0 Hz, 1H), 3.72 (d, J = 5.2 Hz, 9H), 3.63 (t, J = 5.6 Hz, 2H). ^{13}C NMR (101MHz, DMSO-d_6) δ = 150.16, 148.58, 147.85, 134.94, 132.84, 121.34, 121.11, 116.15, 113.10, 105.26, 83.93, 72.38, 60.67, 56.35.

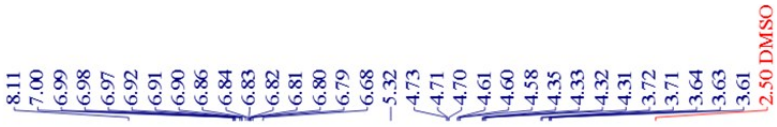

(a)

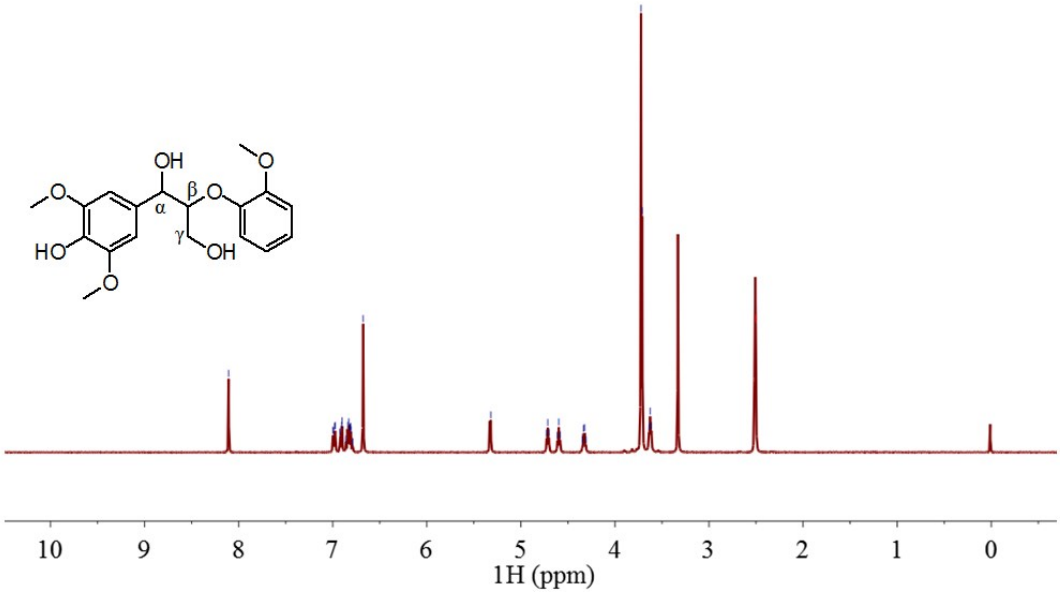

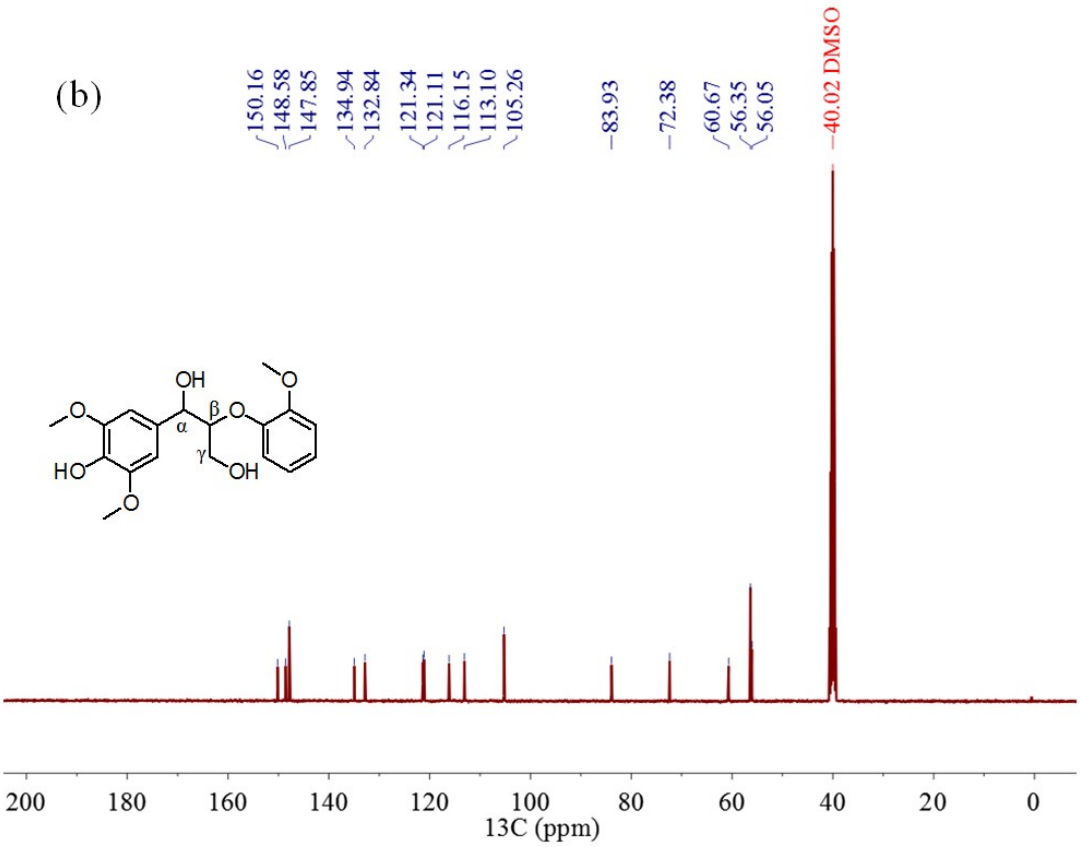

Fig. S6 ^{1}H NMR and ^{13}C NMR spectra of model 5a

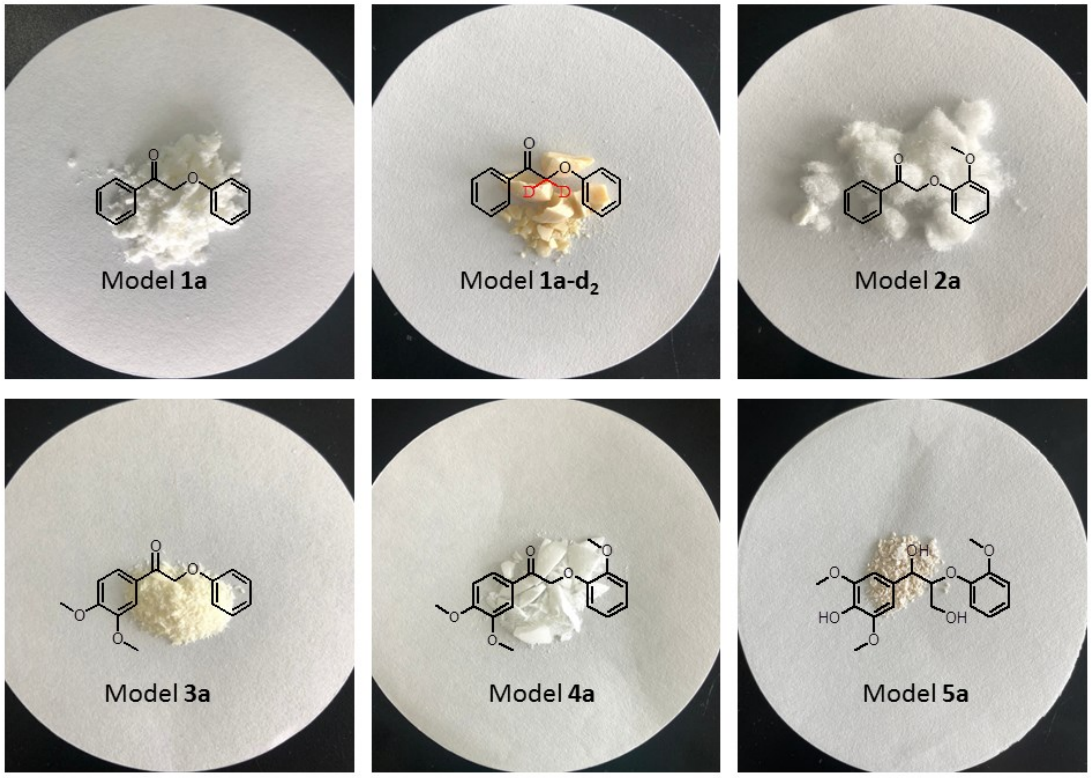

Fig. S7 The synthesized β-O-4 model compounds.

4. Bond dissociation energies (BDEs) of β-O-4 model compounds calculated by density functional theory (DFT)

BDEs were obtained as the difference of the sum of the energies of the dissociated product fragments and the energy of the molecule.

$$BDE=(E_{Frag1} + E_{Frag2})- E_{Mol} \quad (1)$$

where E_{Mol} is the total energy of the molecule, E_{Frag1} and E_{Frag2} are energies of the dissociated products through the selected linkage (either the C-O or C-C linkage). All dissociated fragments were fully optimized.

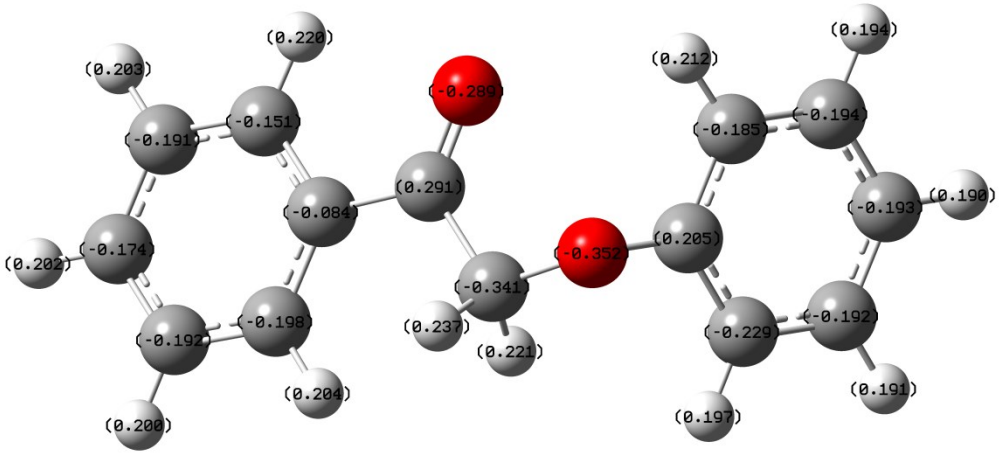

Fig. S8 Optimized structure and Charge distribution of model 1a.

Standard orientation:

Center Number	Atomic Number	Atomic Type	Coordinates (Angstroms) X	Y	Z
1	6	0	-3.995225	-1.304849	-0.431142
2	6	0	-2.694516	-1.147097	0.037367
3	6	0	-2.131487	0.130777	0.143863
4	6	0	-2.893480	1.245296	-0.227425
5	6	0	-4.190174	1.087167	-0.696105
6	6	0	-4.743869	-0.189369	-0.798308
7	1	0	-4.424240	-2.297917	-0.509687
8	1	0	-2.129135	-2.027688	0.318975
9	1	0	-2.442505	2.226170	-0.137543
10	1	0	-4.772605	1.956359	-0.982137

11	1	0	-5.757707	-0.314063	-1.163838
12	6	0	-0.743423	0.366637	0.648995
13	6	0	0.087472	-0.860950	1.040627
14	1	0	0.149696	-1.545209	0.185133
15	1	0	-0.419880	-1.393863	1.849793
16	6	0	2.332679	-0.270388	0.561823
17	6	0	2.822213	1.024399	0.418554
18	6	0	2.851812	-1.313132	-0.203822
19	6	0	3.842239	1.272452	-0.495466
20	1	0	2.380896	1.812928	1.013349
21	6	0	3.864823	-1.053829	-1.123923
22	1	0	2.479303	-2.321905	-0.058861
23	6	0	4.362831	0.238555	-1.272176
24	1	0	4.224982	2.281479	-0.607930
25	1	0	4.272141	-1.866384	-1.716566
26	1	0	5.155183	0.438230	-1.985533
27	8	0	1.367312	-0.521321	1.521675
28	8	0	-0.285749	1.483552	0.750533

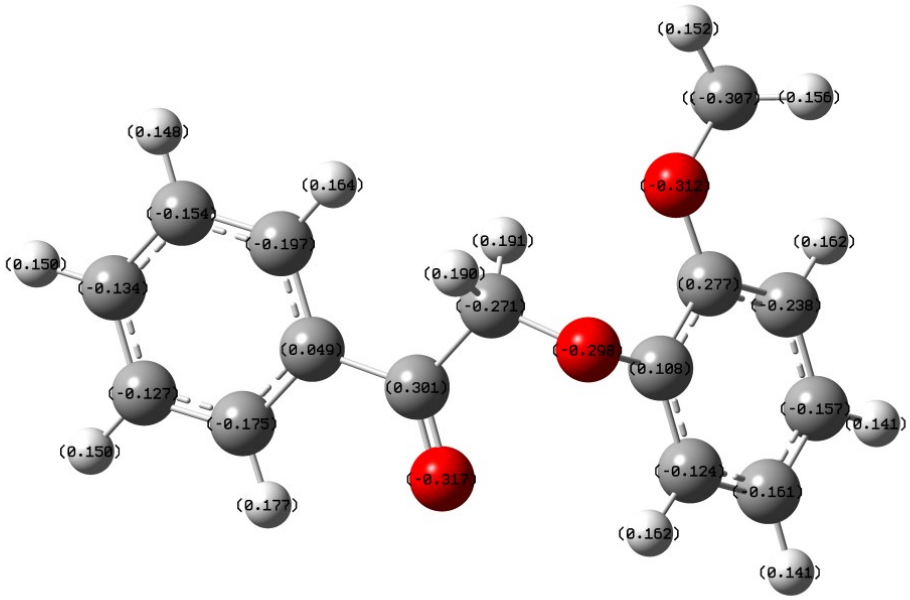

Fig. S9 Optimized structure and Charge distribution of model 2a.

Standard orientation:

Center Number	Atomic Number	Atomic Type	Coordinates (Angstroms) X	Y	Z

1	6	0	4.622562	-0.793158	0.855606
2	6	0	3.367794	-1.179923	0.406071
3	6	0	2.481708	-0.235888	-0.126767
4	6	0	2.877226	1.105429	-0.200921
5	6	0	4.135917	1.492543	0.249244
6	6	0	5.009216	0.545168	0.777817
7	1	0	5.302187	-1.531860	1.266886
8	1	0	3.045045	-2.212907	0.455214
9	1	0	2.211987	1.857129	-0.609383
10	1	0	4.434683	2.533497	0.188237
11	1	0	5.989933	0.848540	1.128988
12	6	0	1.145139	-0.717274	-0.600001
13	6	0	0.197803	0.316827	-1.209012
14	1	0	0.656846	0.730124	-2.111891
15	8	0	-1.033875	-0.243146	-1.615479
16	6	0	-1.957079	-0.476308	-0.619108
17	6	0	-2.332677	-1.780574	-0.336373
18	6	0	-2.576605	0.595359	0.052373
19	6	0	-3.327970	-2.043427	0.603765
20	1	0	-1.816258	-2.574121	-0.860373
21	6	0	-3.561832	0.328201	1.002725
22	6	0	-3.935358	-0.989078	1.273134
23	1	0	-3.614136	-3.067519	0.815727
24	1	0	-4.049234	1.137970	1.530113
25	1	0	-4.706806	-1.179755	2.011502
26	8	0	-2.150907	1.847968	-0.293479
27	6	0	-2.784089	2.958969	0.317645
28	1	0	-3.857528	2.973153	0.102975
29	1	0	-2.631534	2.962957	1.402289
30	1	0	-2.318459	3.842111	-0.115592
31	1	0	0.042552	1.148048	-0.515860
32	8	0	0.827307	-1.883391	-0.511794

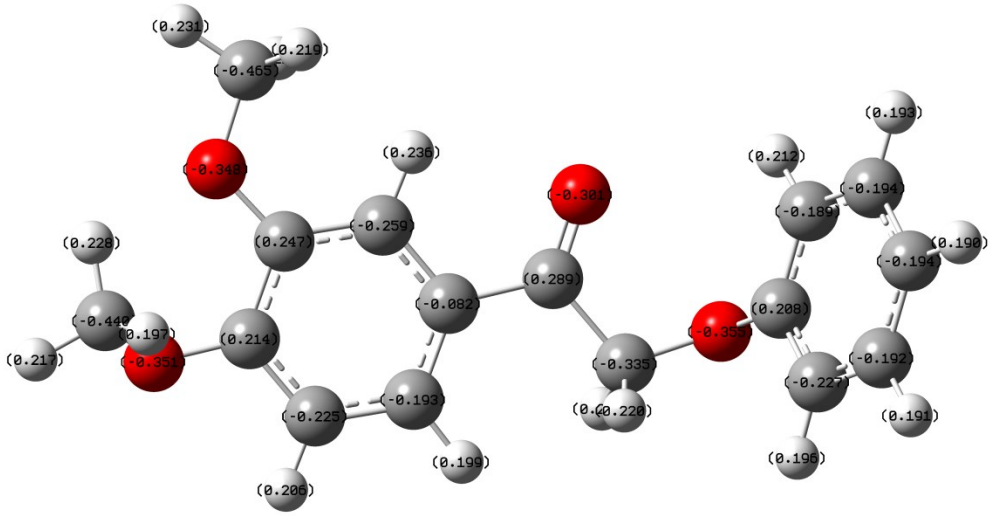

Fig. S10 Optimized structure and Charge distribution of model 3a.

Standard orientation:

Center Number	Atomic Number	Atomic Type	Coordinates (Angstroms) X	Y	Z
1	6	0	-3.093679	0.481053	-0.030816
2	6	0	-1.765112	0.748724	-0.330828
3	6	0	-0.843535	-0.287192	-0.549465
4	6	0	-1.276040	-1.613109	-0.465845
5	6	0	-2.601802	-1.888379	-0.146144
6	6	0	-3.519094	-0.866291	0.080230
7	1	0	-1.398927	1.762717	-0.421279
8	1	0	-0.596590	-2.440260	-0.634777
9	1	0	-2.961744	-2.908237	-0.069905
10	6	0	0.559950	0.103585	-0.876283
11	6	0	1.577053	-1.020992	-1.129144
12	1	0	1.619217	-1.679652	-0.252612
13	1	0	1.239927	-1.625272	-1.976467
14	6	0	3.708312	-0.215467	-0.424143
15	6	0	4.050642	1.118491	-0.213706
16	6	0	4.277133	-1.222212	0.356831
17	6	0	4.969207	1.442039	0.781760
18	1	0	3.578785	1.876315	-0.826086
19	6	0	5.186928	-0.888007	1.358045
20	1	0	4.025972	-2.260024	0.161493
21	6	0	5.535865	0.443766	1.573480

22	1	0	5.236968	2.481344	0.944334
23	1	0	5.632096	-1.672739	1.961681
24	1	0	6.248991	0.701512	2.349674
25	6	0	-3.676236	2.799661	-0.000734
26	1	0	-2.921303	3.091962	0.735874
27	1	0	-3.298091	2.999243	-1.007985
28	1	0	-4.585758	3.373733	0.164756
29	6	0	-5.444699	-0.712050	1.507919
30	1	0	-4.819834	-0.892001	2.388694
31	1	0	-5.657729	0.351891	1.418641
32	1	0	-6.372995	-1.273214	1.604557
33	8	0	-4.810008	-1.223456	0.328580
34	8	0	-4.049595	1.435478	0.149484
35	8	0	0.897686	1.267018	-0.945643
36	8	0	2.857124	-0.532670	-1.468363

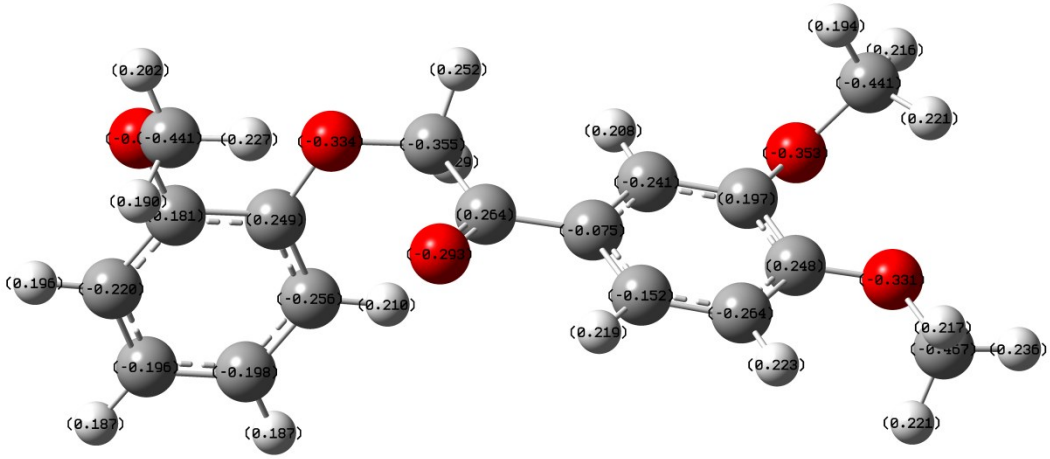

Fig. S11 Optimized structure and Charge distribution of model 4a.

Standard orientation:

Center Number	Atomic Number	Atomic Type	Coordinates (Angstroms) X	Y	Z
1	6	0	3.316629	0.443012	-0.626647
2	6	0	1.958935	0.668433	-0.476711
3	6	0	1.215997	0.012893	0.517223
4	6	0	1.876902	-0.871491	1.371934
5	6	0	3.236770	-1.112768	1.233860

6	6	0	3.970408	-0.468088	0.232765
7	1	0	1.505391	1.367005	-1.169422
8	1	0	1.302559	-1.370513	2.142671
9	1	0	3.720672	-1.812695	1.902309
10	6	0	-0.241278	0.226536	0.708674
11	6	0	-0.955749	1.181168	-0.258262
12	1	0	-0.715123	0.944247	-1.300248
13	1	0	-0.602131	2.198492	-0.070357
14	6	0	-3.100105	0.157899	-0.465728
15	6	0	-4.462711	0.212682	-0.116053
16	6	0	-2.626179	-0.917071	-1.213412
17	6	0	-5.324140	-0.783854	-0.553799
18	6	0	-3.504337	-1.912651	-1.644427
19	1	0	-1.575747	-0.999219	-1.462329
20	6	0	-4.854578	-1.844882	-1.328028
21	1	0	-6.369388	-0.704182	-0.276191
22	1	0	-3.118717	-2.741224	-2.228635
23	1	0	-5.538651	-2.615940	-1.664661
24	6	0	-4.534865	1.267252	1.988559
25	1	0	-4.954812	0.406518	2.520522
26	1	0	-3.447452	1.249124	2.069360
27	1	0	-4.925559	2.188292	2.419742
28	6	0	5.990382	-1.601590	0.806969
29	1	0	5.561810	-2.602648	0.703106
30	1	0	7.012327	-1.604329	0.435068
31	1	0	5.985678	-1.307403	1.860897
32	6	0	4.974761	2.015145	-1.265174
33	1	0	4.537019	2.791599	-0.628817
34	1	0	5.802436	1.532972	-0.743840
35	1	0	5.333118	2.463914	-2.190153
36	8	0	5.291890	-0.658754	0.003811
37	8	0	3.978028	1.063341	-1.650986
38	8	0	-4.955786	1.258911	0.619658
39	8	0	-2.343254	1.219771	-0.047424
40	8	0	-0.862689	-0.310739	1.601257

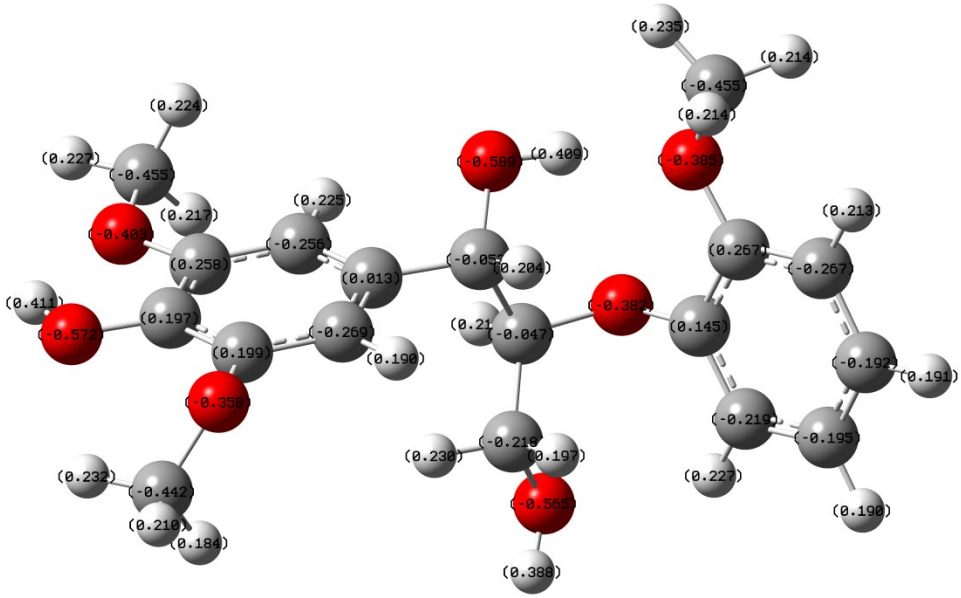

Fig. S12 Optimized structure and Charge distribution of model 5a.

Standard orientation:

Center Number	Atomic Number	Atomic Type	Coordinates (Angstroms) X	Y	Z
1	6	0	-3.452153	-0.900227	0.238868
2	6	0	-2.100250	-1.202525	0.296586
3	6	0	-1.178461	-0.342051	-0.309240
4	6	0	-1.629331	0.802456	-0.954804
5	6	0	-2.990481	1.112121	-1.014547
6	6	0	-3.914247	0.252574	-0.418728
7	1	0	-1.739170	-2.107029	0.765088
8	1	0	-0.939222	1.481296	-1.443987
9	6	0	0.294022	-0.645000	-0.198745
10	1	0	0.830786	-0.094218	-0.985054
11	6	0	0.869987	-0.218416	1.171338
12	1	0	0.354960	-0.789422	1.945926
13	6	0	3.247027	-0.000242	0.650230
14	6	0	3.765431	-0.513079	-0.554175
15	6	0	3.832500	1.122316	1.224402
16	6	0	4.840612	0.123125	-1.172605
17	6	0	4.904949	1.760002	0.602069
18	6	0	5.403541	1.261253	-0.594730
19	1	0	5.248697	-0.263834	-2.097673
20	1	0	5.349766	2.637500	1.058343
21	1	0	6.240282	1.746574	-1.085495

22	8	0	-5.253773	0.503349	-0.490262
23	1	0	-5.701724	-0.226131	-0.039503
24	8	0	2.237852	-0.681921	1.289015
25	6	0	0.698334	1.258210	1.467293
26	1	0	1.258504	1.861868	0.740834
27	1	0	-0.363074	1.500009	1.360545
28	8	0	1.143948	1.509354	2.798438
29	1	0	0.958912	2.431582	3.005782
30	8	0	0.485017	-2.039613	-0.362843
31	1	0	1.436758	-2.188294	-0.260939
32	6	0	-4.119701	-2.885203	1.398041
33	1	0	-3.473627	-2.712822	2.264184
34	1	0	-5.056856	-3.330540	1.725692
35	1	0	-3.616757	-3.558460	0.697747
36	8	0	-4.466430	-1.660390	0.768370
37	6	0	3.463781	-2.068419	-2.355176
38	1	0	2.765065	-2.874091	-2.569707
39	1	0	3.316857	-1.257539	-3.074863
40	1	0	4.489648	-2.442136	-2.426087
41	8	0	3.160862	-1.639951	-1.035699
42	6	0	-4.148554	3.189691	-1.009193
43	1	0	-4.246129	4.043095	-1.679028
44	1	0	-5.134441	2.799942	-0.756348
45	1	0	-3.632571	3.503198	-0.094557
46	8	0	-3.368301	2.224299	-1.718403
47	1	0	3.417909	1.478898	2.158878

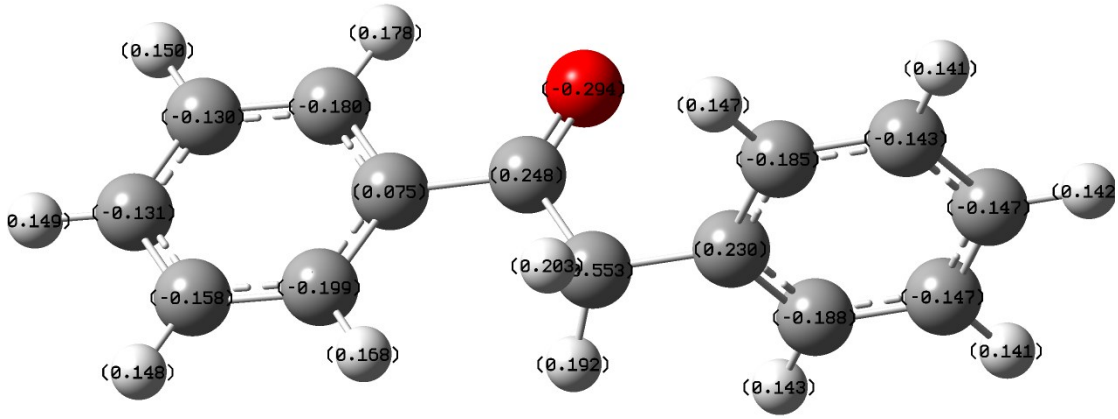

Fig. S13 Optimized structure and Charge distribution of model 1b.

Standard orientation:

Center Number	Atomic Number	Atomic Type	Coordinates (Angstroms) X	Y	Z
1	6	0	-3.859907	-1.299611	0.284583
2	6	0	-2.479008	-1.125793	0.274914
3	6	0	-1.925154	0.126224	-0.016510
4	6	0	-2.779343	1.199806	-0.298210
5	6	0	-4.156287	1.025933	-0.290851
6	6	0	-4.699724	-0.225490	0.001203
7	1	0	-4.280163	-2.273217	0.512888
8	1	0	-1.840137	-1.971661	0.498635
9	1	0	-2.334177	2.162196	-0.519749
10	1	0	-4.809271	1.863554	-0.511661
11	1	0	-5.776014	-0.362486	0.007831
12	6	0	-0.447817	0.381356	-0.037562
13	6	0	0.484921	-0.802961	0.241801
14	1	0	0.227502	-1.614802	-0.446092
15	1	0	0.254076	-1.181533	1.244435
16	6	0	1.944719	-0.459489	0.127994
17	6	0	2.650143	-0.731822	-1.044474

18	6	0	2.613243	0.162602	1.184171
19	6	0	3.996711	-0.396534	-1.159985
20	1	0	2.140593	-1.208633	-1.876765
21	6	0	3.958416	0.499107	1.074477
22	1	0	2.073017	0.390991	2.097952
23	6	0	4.655229	0.219179	-0.099220
24	1	0	4.530988	-0.616945	-2.078394
25	1	0	4.463442	0.981998	1.904690
26	1	0	5.704650	0.480544	-0.186141
27	8	0	-0.011418	1.489369	-0.262703

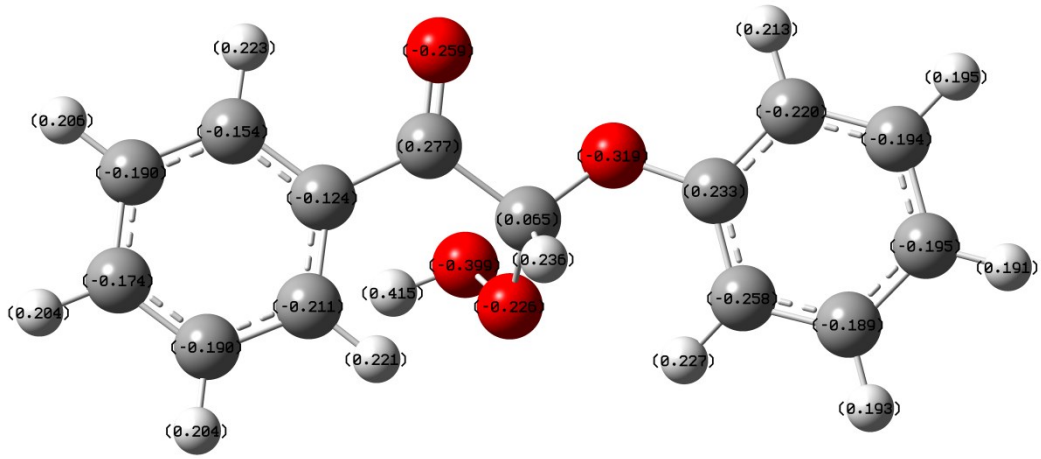

Fig. S14 Optimized structure and Charge distribution of hydroperoxide intermediate h.

Standard orientation:

Center Number	Atomic Number	Atomic Type	Coordinates (Angstroms) X	Y	Z
1	6	0	3.901793	-1.516573	-0.685262
2	6	0	2.604361	-1.039977	-0.518476
3	6	0	2.383080	0.312745	-0.222639
4	6	0	3.483203	1.173540	-0.105721
5	6	0	4.775314	0.693113	-0.263004
6	6	0	4.987496	-0.654800	-0.554076
7	1	0	4.063249	-2.563214	-0.919399
8	1	0	1.773791	-1.726416	-0.612924

9	1	0	3.295254	2.218543	0.108360
10	1	0	5.618958	1.367254	-0.162612
11	1	0	5.997064	-1.031186	-0.680666
12	6	0	1.024887	0.923182	-0.062619
13	6	0	-0.200131	-0.025444	0.013782
14	6	0	-2.558728	0.264143	0.042143
15	6	0	-2.867293	-1.087528	-0.109598
16	6	0	-3.548550	1.236454	-0.102022
17	6	0	-4.174605	-1.452944	-0.431706
18	1	0	-2.115902	-1.846662	0.060996
19	6	0	-4.847737	0.856350	-0.411852
20	1	0	-3.271847	2.276318	0.025294
21	6	0	-5.166813	-0.490905	-0.585266
22	1	0	-4.414418	-2.504766	-0.547438
23	1	0	-5.613445	1.616478	-0.525499
24	1	0	-6.181374	-0.785691	-0.829610
25	8	0	-1.302850	0.739981	0.350018
26	8	0	0.867169	2.117882	-0.022615
27	8	0	0.028092	-1.114232	0.888332
28	8	0	0.529899	-0.584598	2.145529
29	1	0	1.443581	-0.910748	2.122001
30	1	0	-0.351063	-0.530321	-0.950711

5 Supplementary experimental results

5.1 Model compound studies

Table S1 The effect of the amount of base.

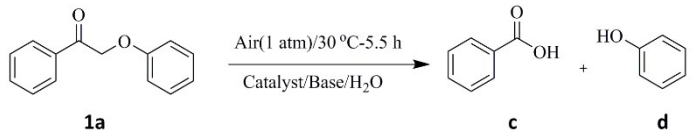

Entry	NaOH (mmol)	Conversion	Yields (C mol%)	
			c	**d**
1	0	0.75	0	0
2	0.1	28.76	6.32	5.53
3	0.2	67.58	35.96	33.64
4	0.4	96.96	85.12	89.03
5	0.5	94.24	78.40	75.41

6	0.8	91.67	49.22	48.48

General conditions: **1a** (0.1 mmol), CuCl catalyst (0.05 mmol), H_2O (2.5 mL), air (1 atm).

Table S2 the effect of temperature and time on the 1a reaction.

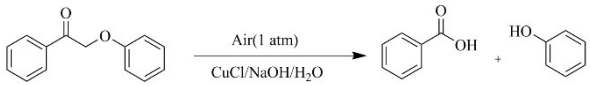

Temperature	Time	Conversion (%)	Yields (mol %)		Selectivity (%)	
			c	**d**	**c**	**d**
30 °C	0.5h	8.11	4.09	4.54	50.43	55.98
	1h	23.55	15.67	16.89	66.54	71.74
	2h	37.30	27.67	30.21	74.18	80.98
	3h	64.69	47.39	49.38	73.26	76.33
	4h	77.60	63.59	69.17	81.95	89.13
	5.5h	96.96	85.12	89.03	87.79	91.83
	6h	100	81.45	83.31	81.45	83.31
	8h	100	74.30	69.65	74.30	69.65
	10h	100	58.36	48.39	58.36	48.39
30 °C	10min	3.53	0	0	0.00	0.00
40 °C		33.76	14.53	17.32	43.04	51.30
50 °C		49.56	32.45	27.88	65.48	56.26
60 °C		65.36	38.09	36.85	58.28	56.38
70 °C		73.38	38.68	32.36	52.71	44.10
80 °C		89.55	33.56	25.15	37.48	28.08
90 °C		100	22.36	16.38	22.36	16.38
100 °C		100	19.55	11.39	19.55	11.39

General conditions: **1a** (0.1 mmol), catalyst (0.05 mmol), NaOH (0.4 mmol), water solvent (2.5 mL), air (1 atm).

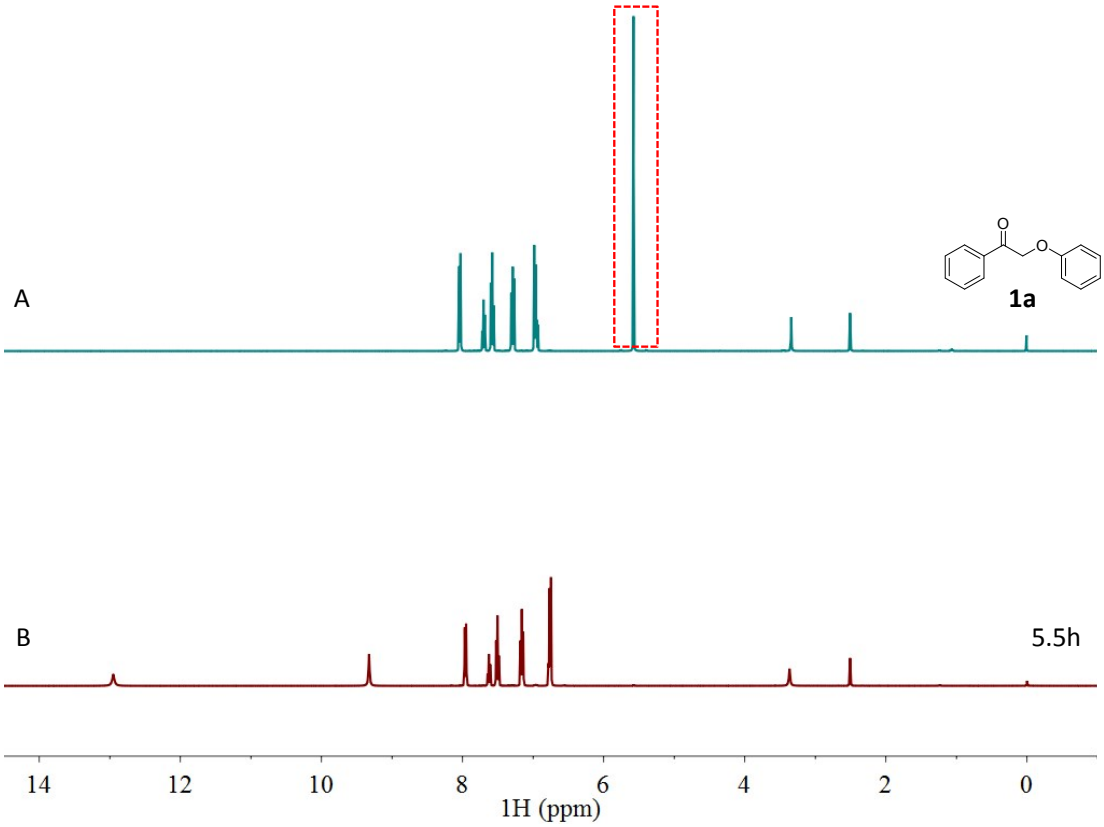

Fig. S15 ^{1}H NMR spectra of (A) model 1a and (B) its oxidative products. Conditions: 1a (0.1 mmol), CuCl (0.05 mmol), NaOH (0.4 mmol), H_2O (2.5 mL), air (1 atm), 30 ºC.

5.2 The conversion of authentic lignin feedstocks

Table S3 Main components of different biomass source

Entry	Biomass source	Cellulose（wt%）	Hemi-cellulose（wt%）	Acid-solluble Lignin （wt%）	Acid-insolluble lignin（wt%）
1	Native corn stover	31.73	21.31	18.15	2.95
2	Native pine wood	43.82	23.22	19.08	3.82
3	Native eucalyptus wood	44.73	13.58	19.27	4.63
4	Native bagasse	44.49	24.20	20.02	2.06
5	Native pennisetum	34.41	16.98	12.46	2.34
6	Bamboo	34.99	19.38	18.36	2.22

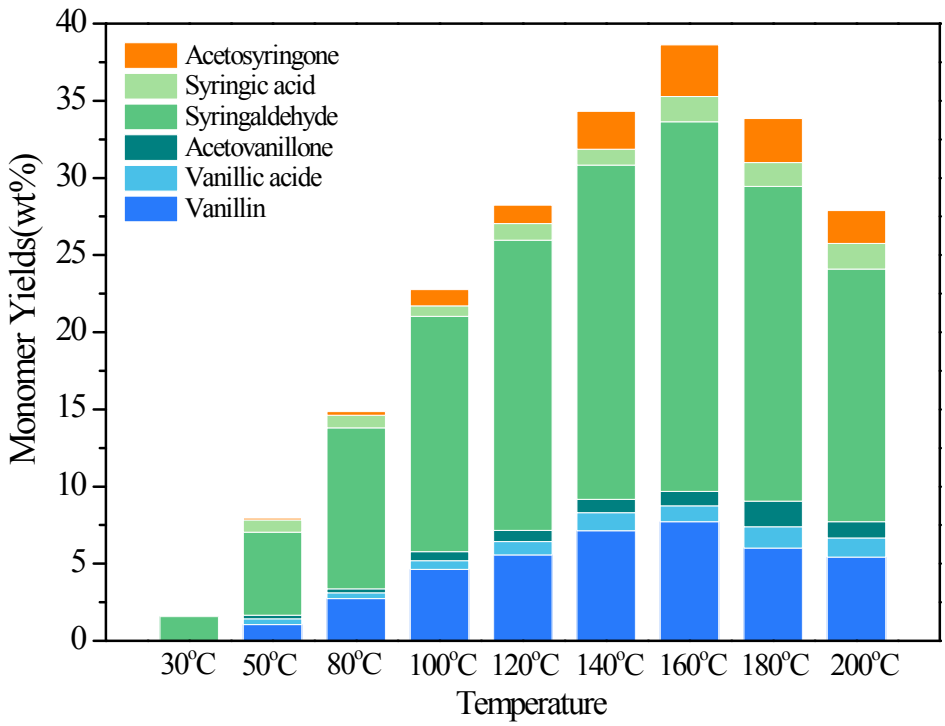

Fig. S16 Effect of temperature on monomer yields (conditions: 0.5 g eucalyptus wood, 0.5 mmol CuCl, NaOH (15 mmol) and H_2O (25 mL) as the solvent, 5 bar air pressure.)

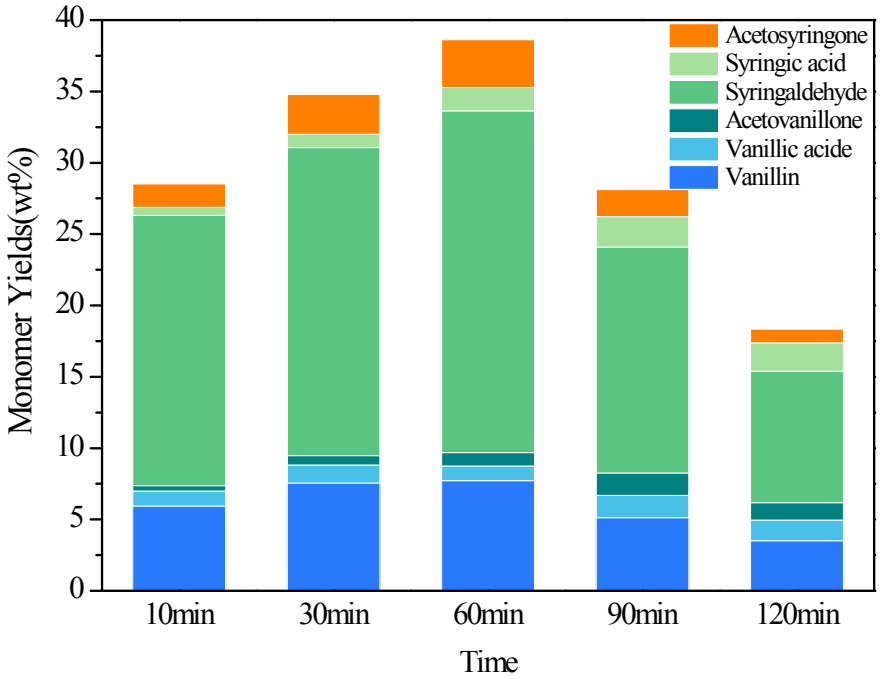

Fig. S17 Effect of reaction time on monomer yields (conditions: 0.5 g eucalyptus wood, 0.5 mmol CuCl, NaOH (15 mmol) and H2O (25 mL) as the solvent, 160 °C，5 bar air pressure.)

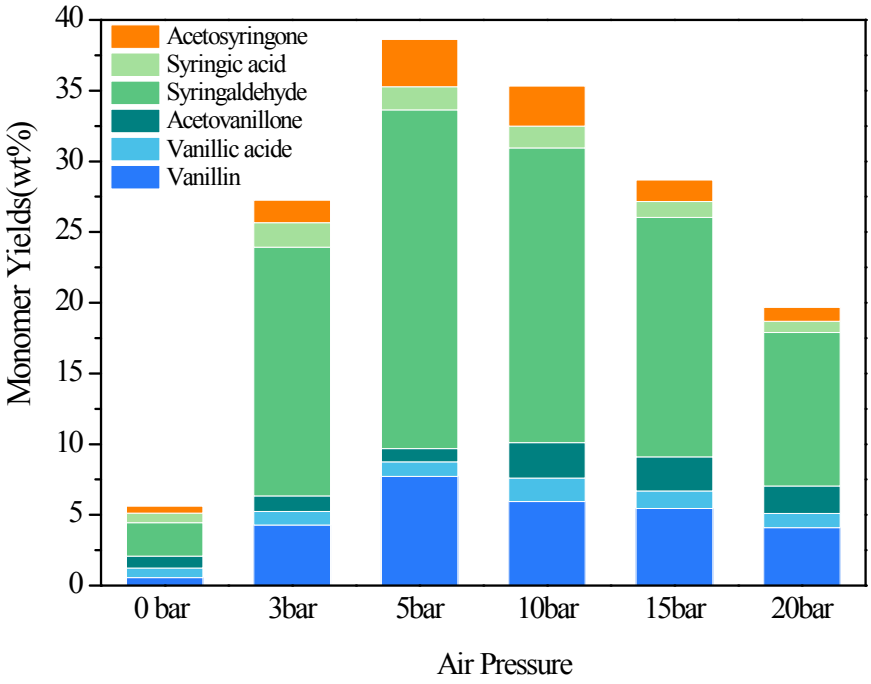

Fig. S18 Effect of initial air pressure on monomer yields (conditions: 0.5 g eucalyptus wood, 0.5 mmol CuCl, NaOH (15 mmol) and H_2O (25 mL) as the solvent, 160 °C，1h.)

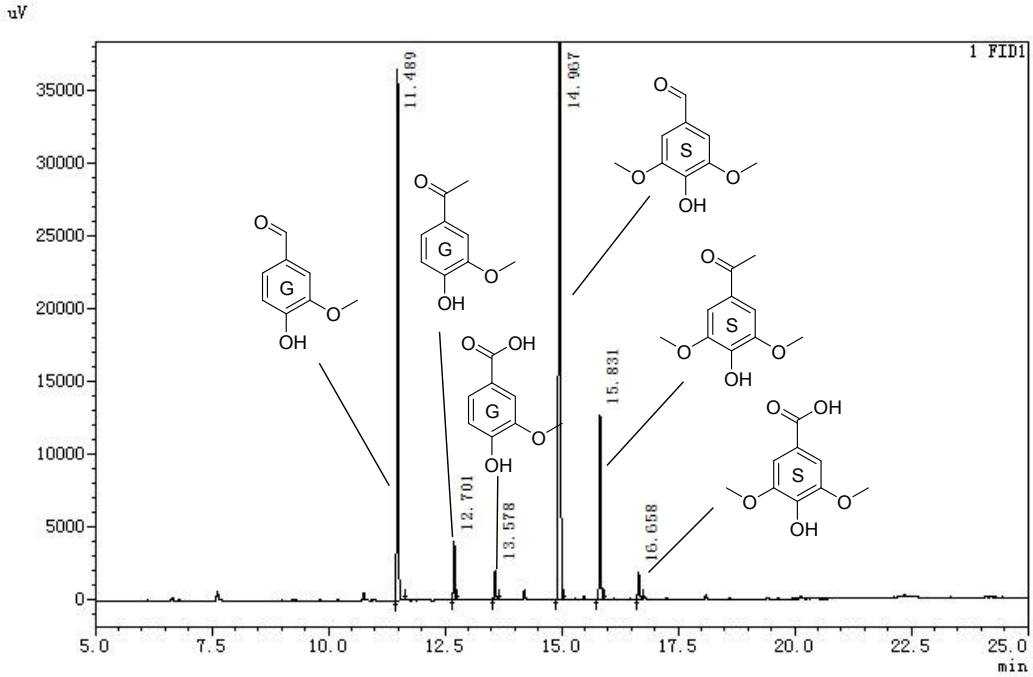

Fig. S19 Gas chromatogram of the monomeric products from eucalyptus oxidation at 160°C for 1h (5 bar air at RT).

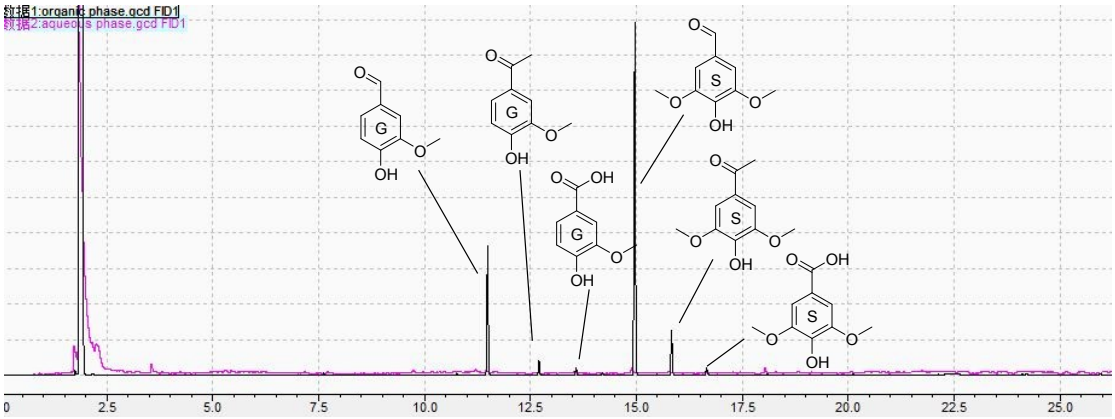

Fig. S20 GC-FID was performed on the aqueous phase after dichloromethane extraction in a typical eucalyptus wood oxidation experiment. The minor peaks corresponding to lignin monomer compounds in the aqueous phase correspond to ~0.1% monomer yield (versus 38.61% in the organic phase), which is negligible.

Table S4 The ascription of lignocellulosic residue infrared absorption band

Entry	Wavenumbers (cm^{-1})	Assignments and comments	Ref
1	2880	C-H stretch in methyl and methylene groups	[3]
2	1425	C–O–H bending in plane at C-6	[4]
3	1370	δC–H	[4]
4	1160	C-O-C at β-glucosidic linkage	[4]
5	1066	C-O at C6	[4]
6	894	C-O-C stretching at β-glycosidic linkage. C-O-C, C-C-O, and C-C-H at C5 and C6	[4]

Table S5 Delignification (%) and Hemicellulose Dissolution (%) of different biomass source in mild alkaline oxidation reaction

Entry	Residue	Delignification(%)	Hemicellulose Dissolution(%)
1	Corn stover	91.23	67.50
2	Pine wood	82.65	60.33
3	Eucalyptus wood	86.67	72.23
4	Bagasse	83.10	61.09
5	Pennisetum	89.36	74.36
6	Bamboo	90.03	77.82

References

1. A. Sluiter, B. Hames, R. Ruiz, C. Scarlata, J. Sluiter, D. Templeton and D. Crocker, Determination of structural carbohydrates and lignin in biomass, Report NREL/TP-5100-60223, National Renewable Energy Laboratory (NREL), Goldon, CO (US), 2008.
2. N. C. Luo, M. Wang, H. J. Li, J. Zhang, T. T. Hou, H. J. Chen, X. C. Zhang, J. M. Lu and F. Wang, Acs Catal, 2017, 7, 4571-4580.
3. S. Y. Oh, D. I. Yoo, Y. Shin, H. C. Kim, H. Y. Kim, Y. S. Chung, W. H. Park and J. H. Youk, Carbohyd Res, 2005, 340, 2376-2391.
4. G. Vazquez, G. Antorrena, J. Gonzalez and S. Freire, Holzforschung, 1997, 51, 158-166.